

The complementary operators method applied to acoustic finite-difference time-domain simulations

John B. Schneider^{a)}

School of Electrical Engineering and Computer Science, Washington State University, Pullman, Washington 99164-2752

Omar M. Ramahi^{b)}

Digital Equipment Corporation PKO3-1/R11, 129 Parker Street, Maynard, Massachusetts 01754

(Received 17 April 1997; revised 2 April 1998; accepted 7 April 1998)

The complementary operators method (COM) has recently been introduced as a mesh-truncation technique for open-domain radiation problems in electromagnetics. The COM entails the construction of two solutions that employ absorbing boundary conditions (ABCs) with complementary behavior, i.e., the reflection coefficients associated with the two ABCs are exactly opposite each other. The average of these solutions then yields a new solution in which the errors caused by artificial reflections from the termination of grid are nearly eliminated. In this work, COM is introduced for the finite-difference time-domain (FDTD) solution of acoustics problems. The development of COM is presented in terms of Higdon's absorbing boundary operators, but generalization to non-Higdon operators is straightforward. The effectiveness of COM in comparison to other absorbing boundary conditions is demonstrated with numerical experiments in two and three dimensions. © 1998 Acoustical Society of America. [S0001-4966(98)01808-6]

PACS numbers: 43.20.Fn, 43.20.Gp, 43.20.Px [JEG]

INTRODUCTION

The finite-difference time-domain (FDTD) method was first introduced by Yee in 1966¹ for the study of electromagnetic scattering problems. A similar method has been developed for simulation of acoustic and elastic wave propagation (e.g., Refs. 2 and 3). The method is simple, both conceptually and in terms of implementation. It is robust and can be used to study accurately a wide range of complex phenomena. Since the FDTD method can be computationally expensive, a great deal of research has been, and continues to be, concerned with finding ways to decrease computational cost, both in memory and run time, while preserving or increasing accuracy. Arguably the most active area of this research is concerned with grid termination techniques for open-domain problem. The way in which the grid is terminated, i.e., the absorbing boundary condition (ABC), often dictates the size of the grid needed to obtain an accurate solution and hence is intimately tied to computational cost. This a consequence of the fact that a simulation employing an ABC of lower accuracy generally requires a larger grid than one employing an ABC of higher accuracy to obtain results of comparable quality.

Most open-domain problems require that the FDTD grid be terminated with an ABC. Open-domain problems need not be terminated with an ABC if a grid can be constructed that is so large that the boundaries of the computational domain are causally isolated from all regions of interest. Unfortunately, this approach is infeasible for nearly all realistic simulations. Global ABCs do exist which are nominally exact (e.g., Ref. 4). However, these ABCs require, for each

terminal point of the grid, an integration over a surface which bounds the interior of the computational domain. Therefore, global ABCs are exceeding costly for time-domain simulations and have not proven to be useful in practical applications. Alternatively, local ABCs merely depend upon the field in the immediate vicinity of each terminal node and are far less costly than global ABCs. However, local ABCs are inherently imperfect and always reflect some spurious energy back into the computational domain. Typically the closer a local ABC is brought to the source of outgoing fields, whether an active element or a scatterer, the greater is the reflected energy (moving the ABC closer to the source of fields implies decreasing the size of the grid). This a consequence of the inability of traditional local ABCs to absorb evanescent energy and the fact that local ABCs typically perform poorly at grazing incidence. Nevertheless, the computational savings afforded by local ABCs outweigh their disadvantages and thus local ABCs are the ones most commonly used today. (In the remainder of the paper only local ABCs are discussed so that the "local" adjective will be dropped.)

There is another distinct approach to the termination of the FDTD grid that relies upon the use of an absorbing material. In such an approach, the absorbing material is placed adjacent to the terminal boundaries. The material is designed to absorb the energy from outgoing waves so that the amount of energy that reenters the interior of the grid via reflection from the grid termination is small. Straightforward material-based termination techniques have been available for several years (see, for example, Refs. 5, 6). An improved technique, employing a nonphysical split-field formulation, was recently presented by Bérenger.⁷ This technique, known as the perfectly matched layer (PML) method, was presented in the context of electromagnetic problems, but it has been adapted

^{a)}Electronic mail: schneidj@eecs.wsu.edu

^{b)}Electronic mail: Omar.Ramahi@digital.com

for acoustic and elastic modeling.^{8–12} The performance of the PML method is such that it has attracted the attention of several researchers. Unfortunately, the quest to improve the PML method has led many researchers to put aside the search for further improvements in differential equation-based ABCs. Nevertheless, as shown here, there are still tremendous improvements that can be made in the application of such ABCs. Thus it is nearly certain that the full potential of both differential equation-based and material-based grid truncation schemes has not yet been realized.

In this paper we provide the theoretical foundation for a new grid truncation technique known as the complementary operators method (COM) and show its application to problems in acoustics. The superiority of the technique over other differential equation-based ABCs is demonstrated via two- and three-dimensional examples. The COM requires that two simulations be performed. In one simulation an ABC is used that reflects energy in a known manner. In the other simulation, the complement of the ABC is used so that the energy reflected by the ABC has the same magnitude but opposite phase. Then, the results of the two simulations are averaged to obtain a solution that is free of most of the energy introduced by ABC reflections. The COM was first presented in the electromagnetics literature where it was shown to yield excellent results even when using a much smaller grid than required by other traditional ABCs.^{13–15} Because of the ease with which the COM can be implemented and the significant impact it can have on accuracy and computational cost, this method has the potential to increase greatly the class of acoustics problems to which FDTD can successfully be applied.

The complementary ABCs (or boundary operators) required by the COM can be formulated from a general class of boundary operators;¹⁵ however, in this paper we present the method specifically in terms of the Higdon ABC.^{16,17} Section I provides a review of Higdon's boundary operators in their differential form and demonstrates the construction of complementary operators of arbitrary order. Section II details the implementation of the COM in the FDTD scheme. Section III provides results from two- and three-dimensional simulations that demonstrate the efficacy of the COM.

Our primary goals here are to present the theory behind the COM and to show the significant advantages it has over other differential equation-based grid truncation methods. Comparison of the COM with other grid termination techniques, such as the PML method, has been investigated elsewhere. The results presented in Refs. 18 and 19 show that the COM can yield results that are superior to the PML method while at the same time being less computationally costly. It should be noted that there is no "best" test with which to compare material-based and differential equation-based grid termination techniques. Instead, many different tests are required to isolate specific aspects of the techniques (e.g., performance at grazing angles, absorption of evanescent energy, and broadband behavior).

Finally, we note that there is an alternative implementation of the COM method to the one presented here.²⁰ The scheme presented in Ref. 20, named the concurrent complementary operators method or C-COM, does not require two

separate simulations, i.e., the complementary boundary operators are realized using a single simulation. The cost associated with this implementation is an increase in memory usage (but that cost "buys" a decrease in total run time). The implementation of a C-COM solution is a straightforward extension to a COM solution and thus this paper concentrates on the basic formulation of COM for acoustic simulations. The reader interested in a concurrent formulation is referred to Ref. 20. We further note that programs that currently employ a Higdon (or Higdon-like) ABC can be modified to use the COM by making changes that are trivial (a simple change of coefficients is all that is required of the existing code and then results must be averaged). To realize a C-COM solution, additional changes must be made to the existing code.

I. DIFFERENTIAL FORM OF BOUNDARY OPERATOR

The first-order, coupled, differential equations governing linear acoustics are

$$\frac{\partial \mathbf{v}}{\partial t} = -\frac{1}{\rho} \nabla p, \quad (1)$$

$$\frac{\partial p}{\partial t} = -c^2 \rho \nabla \cdot \mathbf{v}, \quad (2)$$

where \mathbf{v} is velocity, p is pressure, ρ is density, and c is the speed of sound. The standard FDTD algorithm is obtained by approximating the derivatives in Eqs. (1) and (2) by second-order accurate central differences. The evaluation points for pressure and velocity are spatially and temporally offset from each other so that leapfrog scheme can be constructed to express future fields in terms of past fields (see, for example, Ref. 2 or 8 for details). The usual leapfrog update equations cannot be applied to pressure nodes on the terminal boundary of the computational domain since not all of the needed adjacent fields are available there (i.e., a velocity node is needed that is outside of the grid). Instead, to update these pressure nodes, an auxiliary equation must be used that expresses the boundary value in terms of current or past values of the field in the interior of the grid and past values of the field on the boundary itself. Perhaps the most popular such auxiliary equation is provided by the Higdon boundary operator. The remainder of this section provides the theory behind the differential form of this operator and shows how it can be implemented in a manner suitable for use in the COM. The next section details the discrete form of this operator which, although similar to the continuous operator in many respects, is fundamentally different.

The general M th-order Higdon boundary operator B^M operates on the pressure p at the termination of a computation domain as follows:

$$B^M p = \prod_{m=1}^M B_m p = 0, \quad (3)$$

where

$$B_m = \frac{\partial}{\partial x} + \frac{\xi_m}{c} \frac{\partial}{\partial t} + \alpha_m \quad (4)$$

and ξ_m and α_m are parameters. For arbitrary boundaries, the first partial derivative in Eq. (4) should be taken with respect to the outward normal to the boundary, but the x direction is used here to be consistent with subsequent analysis. Superscripts will be used for the overall order of a boundary operator while a subscript will be used to indicate the constituent components. Thus an individual term B_m is a first-order operator whereas the operator B^M is the M th-order operator obtained from the product $B_1 B_2 \cdots B_M$. When α_m is zero, B_m will yield perfect absorption of plane waves incident at an angle θ_m such that $\xi_m = \cos(\theta_m)$. The parameter α_m was proposed by Higdon as a means of controlling stability of the operator.¹⁷ Additionally, as discussed in Ref. 21, the α_m parameters can be used to absorb evanescent energy (which would otherwise experience unimodular reflection).

Assume that a plane is incident, perhaps obliquely, on a boundary corresponding to a constant x plane. Further assume, without loss of generality, that this boundary corresponds to $x=0$ and over this boundary the Higdon ABC operates on the pressure as given in Eq. (3). The plane wave has unit magnitude and its x component of propagation is in the positive direction. The total pressure in the computational domain will be the superposition of the incident wave and the wave reflected from the boundary

$$p(x, y, z, t) = e^{(j\omega t - jk_x x - jk_y y - jk_z z)} + R^M e^{(j\omega t + jk_x x - jk_y y - jk_z z)}, \quad (5)$$

where k_x , k_y , and k_z (which may be complex) are the x , y , and z components of the wave vector, respectively, ω is frequency, and R^M is the reflection coefficient of the M th-order boundary operator.

The reflection coefficient is obtained by applying Eqs. (3)–(5) and solving for R^M . The result is

$$R^M = (-1)^{M-1} \prod_{m=1}^M R_m(\xi_m, \alpha_m), \quad (6)$$

where

$$R_m(\xi_m, \alpha_m) = -\frac{-jk_x + j\xi_m k + \alpha_m}{jk_x + j\xi_m k + \alpha_m}. \quad (7)$$

As before, the superscript indicates the overall order of the ABC and the subscript indicates constituent components. If the first-order operator B_m were to operate by itself, R_m would be the resulting reflection coefficient. The total reflection coefficient R^M can be obtained from the product of the individual R_m 's [with a sign correction as shown in Eq. (6)].

Consider the reflection coefficient R_M associated with the first-order operator B_M when α_M is zero and when ξ_M either is zero or approaching infinity:

$$R_M(\xi_M=0, \alpha_M=0) = 1, \quad (8)$$

$$\lim_{\xi_M \rightarrow \infty} R_M(\xi_M, \alpha_M=0) = -1. \quad (9)$$

The operator B_M corresponding to Eq. (8) is functionally equivalent to differentiation with respect to x as is evident from inspection of Eq. (4) with ξ and α set to zero. Similarly, the operator corresponding to Eq. (9) is equivalent to differentiation with respect to t . This is clearly seen in the context

of Eq. (3) if both sides are divided by ξ_M prior to taking the limit.

We define M th-order complementary boundary operators as operators whose corresponding reflection coefficients are given by

$$R_0^M = R_M(\xi_M=0, \alpha_M=0) R^{M-1} = -R^{M-1}, \quad (10)$$

$$R_\infty^M = \lim_{\xi_M \rightarrow \infty} R_M(\xi_M, \alpha_M=0) R^{M-1} = R^{M-1}. \quad (11)$$

These operators are labeled B_0^M and B_∞^M , and corresponds to the operators that have $\alpha_M=0$ and ξ_M equal to zero or approaching infinity, respectively. The reflection coefficients of these two M th-order operators are the same in magnitude as the reflection coefficient of an operator of order $M-1$, but, significantly, these reflection coefficients have opposite signs. By performing two simulations, one using B_0^M and once using B_∞^M , and averaging the results, the spurious reflections associated with one ABC will be canceled by the reflections associated with the other ABC. However, as will be discussed below, not all ABC-related errors are eliminated by averaging the two solutions.

One must consider the operators in their finite-difference form, as is done in the next section, rather than their continuous form to understand fully their behavior. For example, since R_∞^M is equal to R^{M-1} , it appears that one of the complementary solutions can be obtained using the reduced-order boundary operator B^{M-1} (i.e., since the reflection coefficients associate with B^{M-1} is R^{M-1} , there is no need to use the higher-order operator B_∞^M). However, when implemented in discrete form, the phase shift associated with $R_M(\xi_M=0, \alpha_M=0)$ is not exactly 180 degrees. The actual phase shift is a function of the coarseness of the grid, the incident angle, and the frequency. The amount that this phase shift differs from the desired value must be accounted for to obtain the most accurate solution possible. As will be shown in the next section, a similar phase shift is produced by the finite-difference equivalent of $\lim_{\xi_M \rightarrow \infty} R_M(\xi_M, \alpha_M=0)$ and this additional term in the operator ensures complete complementarity of the discrete forms of R_0^M and R_∞^M .^{13,15}

Although operators can be used that are exactly complementary in both their continuous and discrete forms, the solution obtained by averaging the two complementary solutions is not completely free of ABC errors. To illustrate this fact, imagine a plane wave obliquely incident on a boundary that is near the corner of the computational domain (it suffices to think of a corner in a two-dimensional problem). In the simulation employing B_0^M the field reflected from the boundary will be scaled by $-R^{M-1}$. If this energy subsequently strikes the other boundary associated with the corner (i.e., the one orthogonal to the first boundary), it will be scaled by $(R^{M-1})^2$. For the simulation employing the B_∞^M boundary operator, the field reflected from the first boundary will be scaled by R^{M-1} . After striking the other boundary, it also will be scaled by $(R^{M-1})^2$. Therefore, when the results are averaged, all the errors associated with a single reflections from the ABCs will cancel while the errors associated with double reflections will add. More generally, errors associated with an odd number of reflections will cancel while

those associated with an even number of reflections will add. This also holds for reflections between the ABC and any scatterer within the computational domain. It should be emphasized that R^{M-1} is typically small so that reducing the error by the square of this amount is substantial.

II. FINITE-DIFFERENCE IMPLEMENTATION

Here we consider the discrete form of the boundary operators described in the previous section. The pressure is assumed to be available at discrete points in space–time and we adopt the standard FDTD notation for those points:

$$p_{i,j,k}^n = p(i\Delta x, j\Delta y, k\Delta z, n\Delta t), \quad (12)$$

where Δx , Δy , and Δz , are the spatial step sizes and Δt is the temporal step size. The operators \mathbf{I} , \mathbf{S} , and \mathbf{T} are defined to be the identity, spatial shift, and temporal shift operators, respectively. Functionally, they perform as follows:

$$\mathbf{I}p_{i,j,k}^n = p_{i,j,k}^n, \quad (13)$$

$$\mathbf{S}p_{i,j,k}^n = p_{i+1,j,k}^n, \quad (14)$$

$$\mathbf{T}p_{i,j,k}^n = p_{i,j,k}^{n+1}. \quad (15)$$

Assuming the last grid point in the x direction is i_{\max} , the discrete form of Eq. (3) that would be applied to the boundary node is

$$\prod_{m=1}^M \left[\frac{\mathbf{I} - \mathbf{S}^{-1}}{\Delta x} \frac{\mathbf{I} + \mathbf{T}^{-1}}{2} + \frac{\xi_m}{c} \frac{\mathbf{I} + \mathbf{S}^{-1}}{2} \frac{\mathbf{I} - \mathbf{T}^{-1}}{\Delta t} + \alpha_m \frac{\mathbf{I} + \mathbf{S}^{-1}}{2} \frac{\mathbf{I} + \mathbf{T}^{-1}}{2} \right] p_{i_{\max},j,k}^{n+1} = 0. \quad (16)$$

This equation is used to obtain $p_{i_{\max},j,k}^{n+1}$ in terms of pressures interior to the grid and previous values of the pressure on the boundary. In order to employ central differences, the discrete form of the boundary operator incorporates spatial and temporal averaging. The reader is referred to Refs. 16 and 17 for further details concerning the implementation of the discrete form of the boundary operator. Carrying out the multiplications and regrouping in terms of the \mathbf{I} , \mathbf{S} , and \mathbf{T} operators, Eq. (16) can be written

$$\prod_{m=1}^M [\mathbf{I} + a_m \mathbf{S}^{-1} + b_m \mathbf{T}^{-1} + c_m \mathbf{S}^{-1} \mathbf{T}^{-1}] p_{i_{\max},j,k}^{n+1} = 0, \quad (17)$$

where

$$a_m = \frac{-1 + \xi_m \Delta x / c \Delta t + \alpha_m \Delta x / 2}{1 + \xi_m \Delta x / c \Delta t + \alpha_m \Delta x / 2}, \quad (18)$$

$$b_m = \frac{1 - \xi_m \Delta x / c \Delta t + \alpha_m \Delta x / 2}{1 + \xi_m \Delta x / c \Delta t + \alpha_m \Delta x / 2}, \quad (19)$$

$$c_m = \frac{-1 - \xi_m \Delta x / c \Delta t + \alpha_m \Delta x / 2}{1 + \xi_m \Delta x / c \Delta t + \alpha_m \Delta x / 2}. \quad (20)$$

The finite-difference equivalent of Eqs. (3) and (4) are thus

$$\tilde{B}^M p_{i_{\max},j,k}^{n+1} = \prod_{m=1}^M \tilde{B}_m p_{i_{\max},j,k}^{n+1} = 0, \quad (21)$$

where

$$\tilde{B}_m = \mathbf{I} + a_m \mathbf{S}^{-1} + b_m \mathbf{T}^{-1} + c_m \mathbf{S}^{-1} \mathbf{T}^{-1}. \quad (22)$$

The tildes distinguish the discrete operators from the continuous ones. Now consider the discrete form of Eq. (5)

$$p_{i,j',k}^n = e^{(j\omega n\Delta t - j\tilde{k}_x i\Delta x - j\tilde{k}_y j'\Delta y - j\tilde{k}_z k\Delta z)} + \tilde{R}^M e^{(j\omega n\Delta t + j\tilde{k}_x i\Delta x - j\tilde{k}_y j'\Delta y - j\tilde{k}_z k\Delta z)}. \quad (23)$$

A prime has been added to the spatial index in the y direction to distinguish it from the symbol j used to represent $\sqrt{-1}$. The tilde on wave vector components emphasizes that the numeric wave vector differs from the continuous one since the dispersion relation in an FDTD grid differs slightly from the true one.

Using Eq. (23) in (21) and, without loss of generality, letting i_{\max} equal zero, one can solve for the numeric reflection coefficient \tilde{R}^M

$$\tilde{R}^M = (-1)^{M-1} \prod_{m=0}^M \tilde{R}_m(\xi_m, \alpha_m), \quad (24)$$

where

$$\tilde{R}_m(\xi_m, \alpha_m) = - \frac{1 + a_m e^{j\tilde{k}_x \Delta x} + b_m e^{-j\omega \Delta t} + c_m e^{j\tilde{k}_x \Delta x - j\omega \Delta t}}{1 + a_m e^{-j\tilde{k}_x \Delta x} + b_m e^{-j\omega \Delta t} + c_m e^{-j\tilde{k}_x \Delta x - j\omega \Delta t}}. \quad (25)$$

As with the continuous operators, \tilde{R}_m is the reflection coefficient obtained when using the first-order operator \tilde{B}_m by itself and \tilde{R}^M is the product of the \tilde{R}_m 's with a correction made for the sign.

Motivated by the analysis of the previous section, we consider \tilde{R}_M when α_M is zero and ξ_M is either zero or approaching infinity. However, since Eq. (25) gives \tilde{R}_M in terms of a_M , b_M , and c_M , it is helpful first to obtain these coefficients directly from Eqs. (18) to (20). For the two cases of interest here, the sets of coefficients are

$$\tilde{R}_M(\xi_M=0, \alpha_M=0) \Rightarrow a_M = -1; \quad b_M = 1; \quad c_M = -1, \quad (26)$$

$$\lim_{\xi_M \rightarrow \infty} \tilde{R}_M(\xi_M, \alpha_M=0) \Rightarrow a_M = 1; \quad b_M = -1; \quad c_M = -1. \quad (27)$$

Using these in Eq. (25) yields

$$\tilde{R}_M(\xi_M=0, \alpha_M=0) = \exp(j\tilde{k}_x \Delta x), \quad (28)$$

$$\lim_{\xi_M \rightarrow \infty} \tilde{R}_M(\xi_M, \alpha_M=0) = -\exp(j\tilde{k}_x \Delta x). \quad (29)$$

As was the case for the continuous operators (Refs. 8 and 9), these two reflection coefficients are exactly complementary. The discrete form of Eqs. (10) and (11) is thus

$$\tilde{R}_0^M = \tilde{R}_M(\xi_M=0, \alpha_M=0) \tilde{R}^{M-1} = -\exp(j\tilde{k}_x \Delta x) \tilde{R}^{M-1}, \quad (30)$$

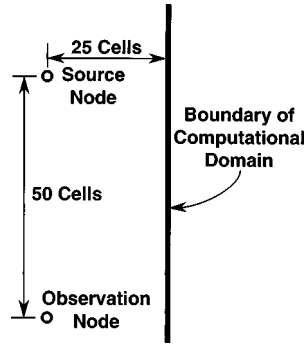


FIG. 1. Sketch of geometry used to test numerical complementarity. The boundary is terminated using either \tilde{B}_0^2 or \tilde{B}_∞^2 . Boundaries other than the one shown are sufficiently far away so that no energy is reflected by them over the duration of the simulation. The reference solution is obtained with the same spacing between the source and observation point, but all boundaries are causally isolated from the observation point.

$$\tilde{R}_\infty^M = \lim_{\xi_M \rightarrow \infty} \tilde{R}_M(\xi_M, \alpha_M = 0) \tilde{R}^{M-1} = \exp(j\tilde{k}_x \Delta x) \tilde{R}^{M-1}, \quad (31)$$

which have the corresponding boundary operators \tilde{B}_0^M and \tilde{B}_∞^M given by

$$\tilde{B}_0^M = [\mathbf{I} - \mathbf{S}^{-1} + \mathbf{T}^{-1} - \mathbf{S}^{-1} \mathbf{T}^{-1}] \prod_{m=1}^{M-1} [\mathbf{I} + a_m \mathbf{S}^{-1} + b_m \mathbf{T}^{-1} + c_m \mathbf{S}^{-1} \mathbf{T}^{-1}], \quad (32)$$

$$\tilde{B}_\infty^M = [\mathbf{I} + \mathbf{S}^{-1} - \mathbf{T}^{-1} - \mathbf{S}^{-1} \mathbf{T}^{-1}] \prod_{m=1}^{M-1} [\mathbf{I} + a_m \mathbf{S}^{-1} + b_m \mathbf{T}^{-1} + c_m \mathbf{S}^{-1} \mathbf{T}^{-1}]. \quad (33)$$

It is important to note, as is clear from Eqs. (30) and (31), that these two discrete boundary operators are, as were the continuous operators, exactly complementary. The fact that complementarity is also preserved numerically (i.e., when implemented using finite-precision arithmetic) will be shown in the next section.

III. NUMERICAL RESULTS

In this section two problems are considered to study the behavior of the ABCs. The first is simply propagation in a homogeneous region while the second is propagation about a pressure-release (Dirichlet boundary condition) sphere. Although analytic solutions are available for both these problems, comparisons are made to reference solutions also obtained from FDTD simulations. If results were compared to analytic solutions, numerical artifacts inherent in the FDTD technique other than those caused by the grid termination (e.g., grid dispersion) could make meaningful interpretation difficult. Hence, the FDTD reference solutions, which use large grids to eliminate boundary errors over the duration of the simulations, permit the ABC errors to be separated from any other numeric artifacts.

First we demonstrate that the numerical implementation of \tilde{B}_0^M and \tilde{B}_∞^M yields complementary results even when the error associated with the individual operators is large. Consider the two-dimensional problem depicted in Fig. 1 which

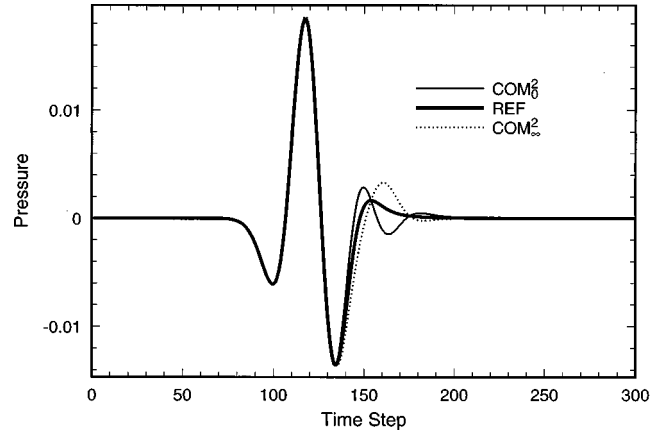


FIG. 2. Pressure at the observation point. The units of pressure here, as in all other plots, can be chosen arbitrarily.

is, ideally, the equivalent of a point source (three-dimensional line source) radiating in a homogeneous medium. The source is realized by adding a Ricker wavelet to the update equations for the source node. (This yields a transparent source that introduces fields into the computational domain without scattering them. See Ref. 22 for further discussion of the implementation of transparent sources.) The maximum value of the source function is unity (arbitrary units). The discretization is such that the peak frequency of the wavelet is sampled at 32 points per wavelength. The Courant number ($c\Delta t/\Delta x$) is 0.95 times the two-dimensional limit of $1/\sqrt{2}$ and the spatial step size is the same throughout the grid. Three simulations were performed. In the first, the boundary operator was \tilde{B}_0^2 with $\xi_1 = 1$ and $\alpha_1 = 0$ (these parameters will provide perfect absorption for a plane wave normally incident on the boundary); in the second, the boundary operator was \tilde{B}_∞^2 with, again, $\xi_1 = 1$ and $\alpha_1 = 0$; the third simulation was a reference solution in which all the boundaries of the computational domain were causally isolated from the observation point over the duration of the simulation. We label the results from these three simulations COM_0^2 , COM_∞^2 , and REF.

Figure 2 shows the results of the three simulations recorded over 300 time steps. Note that the solutions obtained using \tilde{B}_0^2 and \tilde{B}_∞^2 differ substantially from the reference solution. The errors are comparable to that of a first-order Higdon ABC by itself (the errors differ only in phase). To show that the error in the two ABC-terminated solutions are complementary, Fig. 3 shows plots of the difference between the reference solution and the complementary solutions, i.e., plots of the error in the two solutions. Note that these error plots appear to be exactly opposite each other. The ultimate COM solution for this problem, which we label COM^2 , is the average of the two complementary run; thus at each time step $\text{COM}^2 = (\text{COM}_0^2 + \text{COM}_\infty^2)/2$. A plot of COM^2 is indistinguishable from the reference solution and does not warrant a separate figure. Instead, it is instructive to plot the error in COM^2 . Figure 4 shows the logarithm (base 10) of the absolute value of the difference between REF and COM^2 as a function of time. The significance of this plot is that the difference between the two solutions hovers around the numeric noise floor for double precision numbers. (Double pre-

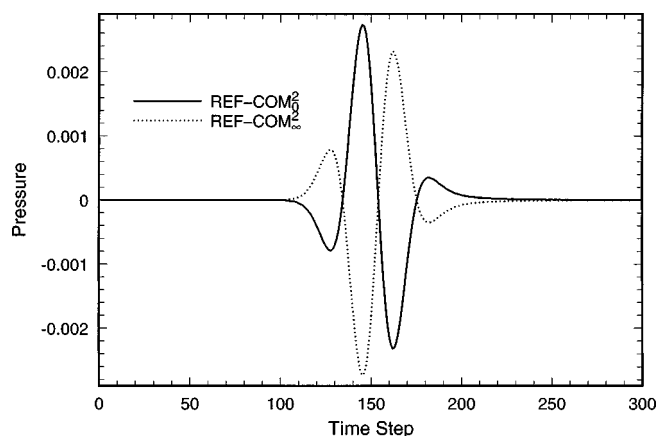


FIG. 3. Difference between the reference solution and the two solutions that used complementary boundary operators.

cision arithmetic yields between 14 and 15 digits of precision. Given that the peak value of the observed pressure has a magnitude of approximately 10^{-2} , the numeric noise floor should be in the range of 10^{-16} to 10^{-17} . This is precisely the range of errors seen in Fig. 4.) We must add, however, that this problem was constructed so that there are no multiple reflections. As was mentioned at the end of Sec. I, the ABC-induced errors associated with an even numbers of multiple reflections add rather than cancel.

To demonstrate the performance of the COM in three dimensions, we consider the pressure about a pressure-release sphere (i.e., the Dirichlet boundary condition is enforced over the surface of the sphere) that is insonified by an isotropic point source. This problem is designed to provide a stringent environment for testing the performance of ABCs and is not, per se, designed to provide a realistic model of any particular physical system. Thus this study was performed all in terms of nondimensional units, e.g., the number of points per wavelength and the Courant number.

The computational domain is 39 cells \times 39 cells \times 39 cells; the sphere has a radius of ten cells and is centered in the computation space. The spatial step sizes are the same in all directions, i.e., $\Delta x = \Delta y = \Delta z = \delta$. The Courant number, $c\Delta t/\delta$ is $1/\sqrt{3}$ which is approximately 98% of the three-dimensional limit. Figure 5 shows a slice through the middle of the computational domain. (Although drawn as a

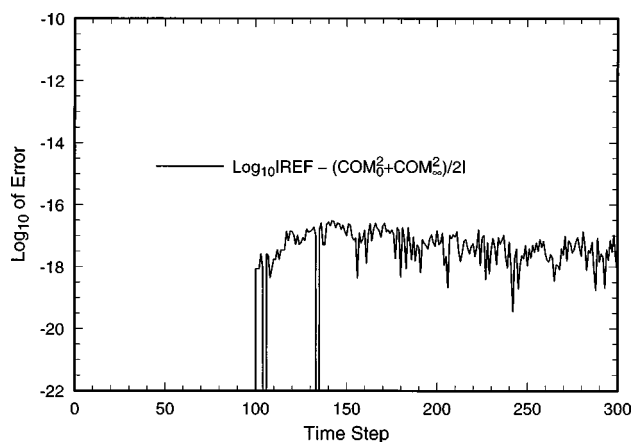


FIG. 4. Log base 10 of the error in the COM solution.

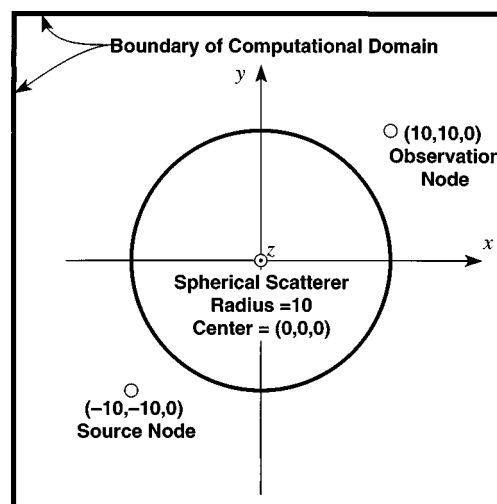


FIG. 5. Cross section of three-dimensional problem showing the source and observation points. Coordinates are relative to the center of the sphere. The boundary is terminated using either \tilde{B}_0^4 or \tilde{B}_∞^4 . The reference solution is obtained using a large grid that causally isolated the boundaries from the observation point over the duration of the simulation.

continuous circle, the actual boundary of the spherical scatterer follows the staircased boundary inherent in Cartesian-cell FDTD simulations.) The source node is a pressure node where the pressure is given by a Ricker wavelet. However, unlike before, the usual update equation does not apply at this one node. In that sense the source node itself is “hard,” i.e., it will scatter any field incident upon it. The discretization is such that there are 20 points per wavelength at the peak spectral content of the wavelet. Hence, the diameter of the sphere corresponds to one wavelength of the most energetic portion of the insonification. The locations of the source and observation points are as shown in Fig. 5. Since the observation point is on the opposite side of the sphere from the source and the boundary of the computational domain is, at its closest point, only nine cells away from the sphere, the quality of the ABC significantly influences the observed field. Since the fields at the observation point are small relative to the peak amplitude of the source pulse, the source function was scaled by a factor of 5000. This was done solely to facility plotting and, since the units of pressure can be chosen arbitrarily, has no effect on the interpretation of the results.

The boundary is terminated either using \tilde{B}_0^4 , \tilde{B}_∞^4 , or \tilde{B}^4 . We label the associated solutions COM_0^4 , COM_∞^4 , and HIG^4 , respectively. (The HIG^4 solution is that which is obtained using the standard fourth-order Higdon ABC.) The solution obtained by the average of COM_0^4 and COM_∞^4 is labeled COM^4 . The parameter α_m was zero for all the first-order constituent components of these boundary operators, while ξ_m was unity (except, of course, where ξ was used to establish complementary behavior in \tilde{B}_0^4 and \tilde{B}_∞^4). Thus no attempt was made to “tune” the ABC parameters to the particular problem at hand or optimize the coefficient for a general problem. However, it should be noted that if a set of parameters can be found that improves the performance of the Higdon ABC, the benefit realized by using the same set of parameters in a COM formulation should be even greater (i.e.,

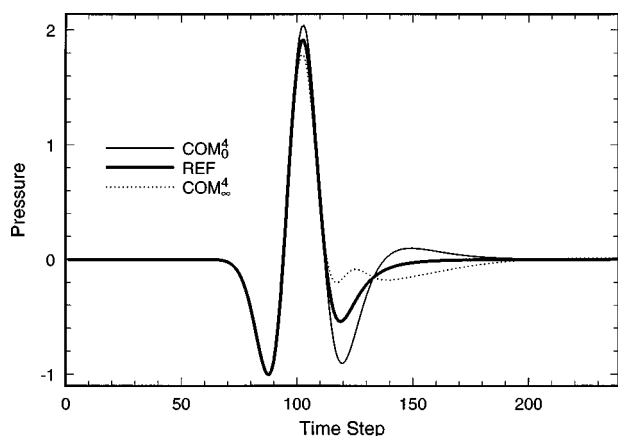


FIG. 6. Pressure at observation point obtained using either the boundary operator \tilde{B}_0^4 (COM_0^4) or \tilde{B}_∞^4 (COM_∞^4). The reference solution is free of all ABC errors.

the square of that realized using an uncomplemented formulation).

Note that the reflection coefficients, and hence the ABC-induced errors, for the COM_0^4 and COM_∞^4 solutions are comparable to that of a third-order Higdon ABC. The reflection coefficient for the HIG^4 solution, on the other hand, is the smaller reflection coefficient of the fourth-order Higdon ABC. But, all these solutions require the same computational resources in terms of backstorage of fields and number of operations—they only differ in the coefficients used in the boundary-node update equations. Given the size of the reflection coefficient in each simulation, the HIG^4 should give better results than either COM_0^4 or COM_∞^4 individually. However, the import question is: How does HIG^4 compare to COM^4 ?

Figure 6 shows the reference solution (obtained using a large grid which is free of all ABC errors) together with COM_∞^4 and COM_0^4 . There are obvious and significant errors, but, given the design of this “test bed,” the errors are not surprising. Figure 7 shows the reference solution together with HIG^4 and COM^4 . As anticipated, HIG^4 is more accurate than either COM_0^4 or COM_∞^4 . However, COM^4 is obviously

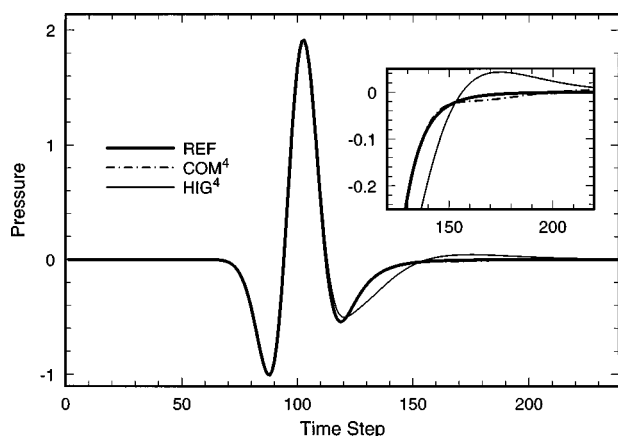


FIG. 7. Pressure at observation point obtained using the average of the two complementary results (COM^4) and obtained using a Higdon fourth-order operator (HIG^4). The inset box shows the pressure from time step 120 to 220 with the vertical scale magnified by a factor of 10.

more accurate than HIG^4 . Since it is difficult to tell the difference between the reference solution and COM^4 when plotting the entire pulse, an inset shows a plot of the trailing portion of the pulse with the vertical scale magnified by approximately ten. On this scale the slight errors in COM^4 can be seen.

IV. CONCLUSIONS

By averaging the results obtained from two simulations in which complementary boundary operators are used, ABC-related errors can be significantly reduced. The final result is superior to that which can be obtained using a higher-order ABC by itself. The construction of complementary operators is relatively simple. In fact, any acoustic code which currently employs a Higdon ABC can be modified with little effort to use complementary operators. One merely has to employ different sets of coefficients for the boundary update equations (i.e., other than a change of constants, no other modifications are needed). The cost of using the COM is that two simulations must be performed. However, given the quality of the results obtained, this cost can be more than offset by the use of a smaller computational domain (see Ref. 15 for a discussion of this point). Additionally, in situations where one is willing to trade an increase in memory for a reduction in total computation time, a concurrent-COM scheme has been presented elsewhere.²⁰

As demonstrated here, the COM applies equally well to two- and three-dimensional acoustics problems. It is further anticipated that the complementary operators method can be applied to problems in elastic propagation and this will be the subject of future investigations.

ACKNOWLEDGMENT

This work was supported by Digital Equipment Corporation and the Office of Naval Research, Code 3210A.

- ¹K. S. Yee, “Numerical solution of initial boundary value problems involving Maxwell’s equations in isotropic media,” *IEEE Trans. Antennas Propag.* **14**, 302–307 (1966).
- ²D. Botteldooren, “Acoustical finite-difference time-domain simulation in a quasi-Cartesian grid,” *J. Acoust. Soc. Am.* **95**, 2313–2319 (1994).
- ³J. Virieux, “P-SV wave propagation in heterogeneous media: Velocity-stress finite difference method,” *Geophysics* **51**, 889–901 (1986).
- ⁴J. De Moerloose and D. De Zutter, “Surface integral representation radiation boundary condition for the FDTD method,” *IEEE Trans. Antennas Propag.* **41**, 890–896 (1993).
- ⁵R. Holland and J. W. Williams, “Total-field versus scattered-field finite-difference codes: A comparative assessment,” *IEEE Trans. Nucl. Sci.* **NS-30**, 4583–4588 (1983).
- ⁶C. Cerjan, D. Kosloff, R. Kosloff, and M. Reshef, “A nonreflecting boundary condition for discrete acoustic and elastic wave equations,” *Geophysics* **50**, 705–708 (1985).
- ⁷J.-P. Berenger, “A perfectly matched layer for the absorption of electromagnetic waves,” *J. Comput. Phys.* **114**, 185–200 (1994).
- ⁸J. G. Maloney and K. E. Cummings, “Adaptation of FDTD techniques to acoustic modeling,” in *11th Annual Review of Progress in Applied Computational Electromagnetics*, Vol. 2 (Monterey, CA), pp. 724–731, Mar. 1995.
- ⁹F. D. Hastings, J. B. Schneider, and S. L. Broschat, “Application of the perfectly matched layer (PML) absorbing boundary condition to elastic wave propagation,” *J. Acoust. Soc. Am.* **100**, 3061–3069 (1996).
- ¹⁰W. C. Chew and Q. H. Liu, “Perfectly matched layers for elastodynamics:

- A new absorbing boundary condition," *J. Comput. Acoust.* **4**, 341–359 (1996).
- ¹¹X. Yuan, D. Borup, J. W. Wiskin, M. Berggren, R. Eidsen, and S. A. Johnson, "Formulation and validation of Berenger's PML absorbing boundary for the FDTD simulation of acoustic scattering," *IEEE Trans. Ultrason. Ferroelectr. Freq. Control* **44**, 816–822 (1997).
 - ¹²Q. H. Liu and J. Tao, "The perfectly matched layer for acoustic waves in absorptive media," *J. Acoust. Soc. Am.* **102**, 2072–2082 (1997).
 - ¹³O. Ramahi, "Application of the complementary operator method to the finite-difference–time domain solution of the three-dimensional radiation problem," *Microwave Opt. Technol. Lett.* **9**, 147–149 (1995).
 - ¹⁴O. M. Ramahi, "Complementary operators: A method to annihilate artificial reflections arising from the truncation of the computational domain in the solution of partial differential equations," *IEEE Trans. Antennas Propag.* **43**, 697–704 (1995).
 - ¹⁵O. M. Ramahi, "Complementary boundary operators for wave propagation problems," *J. Comput. Phys.* **133**, 113–128 (1997).
 - ¹⁶R. L. Higdon, "Absorbing boundary conditions for difference approximations to the multi-dimensional wave equation," *Math. Comput.* **47**, 437–459 (1986).
 - ¹⁷R. L. Higdon, "Numerical absorbing boundary conditions for the wave equation," *Math. Comput.* **49**, 65–90 (1987).
 - ¹⁸J. Schneider and O. M. Ramahi, "A comparison and evaluation of the PML and COM mesh truncation techniques for FDTD simulation," in *IEEE Antennas and Propagat. Soc. Int. Symp.* (Montréal, Canada), Vol. 3, pp. 1904–1907, July 1997.
 - ¹⁹O. M. Ramahi and J. B. Schneider, "Comparative study of the PML and C-COM mesh-truncation techniques," *IEEE Microwave Guid. Wave Lett.* **8**, 55–57 (1998).
 - ²⁰O. M. Ramahi, "Concurrent implementation of the complementary operators method in 2-D space," *IEEE Microwave Guid. Wave Lett.* **7**, 165–167 (1997).
 - ²¹J. Fang, "Absorbing boundary conditions applied to model wave propagation in microwave integrated-circuits," *IEEE Trans. Microwave Theory Tech.* **42**, 1506–1513 (1994).
 - ²²J. B. Schneider, C. L. Wagner, and S. L. Broschat, "Implementation of transparent sources embedded in acoustic finite-difference time-domain grids," *J. Acoust. Soc. Am.* **103**, 136–142 (1998).